Busbar Differential Protection Using an Alternative Generalized Alpha Plane

F. A. M. Vásquez, K. M. Silva

***Abstract*—This paper describes an alternative busbar differential protection function based on the generalized alpha plane. This approach faithfully maps several currents in two equivalent currents such that it preserves the original restraint and operation signals. The original formulation was applied to multi-terminal transmission lines protection but the number of terminals can be small if compared with the number of bays connected to busbars. For this reason, this first method is initially assessed in order to verify its suitability for busbar protection purposes. After that, an alternative algorithm to map the currents in the same plane is described and tested by using a double-bus-single-breaker 220 kV busbar configuration, modeled in ATPdraw. The simulations of internal and severe external faults, as well as evolving faults, are performed for a wide variety of scenarios including fault times, fault resistances and fault types. The results bring up a greater robustness and shorter response time if compared with original alpha plane approach, thus it represents an alternative as a busbar protection function which provides high reliability and it can be easily implemented in a commercial relay due to its mathematical simplicity.**

***Keywords*—Busbars, alpha plane, differential protection, ATPdraw.**

I. Introduction

The major concerns of modern busbar protection are fast operation time for internal faults, security in case of external faults with current transformer (CT) saturation and adaptability in case of evolving faults [1]. These challenges are traditionally addressed with high-impedance and low-impedance schemes, which are differentiated by the burden connected to CTs. Even though the first method is immune to CT saturation, the second one easily facilitates the sharing of CTs with different transformation ratios as well as to modify the CT polarity via software. Also, it can deal with dynamic busbar arrangements by integrating a protection zones logic [2].

The researches related to new busbar protection functions has increased in last five years. In order to describe them, the Table I summarizes these techniques, as well as their decision times, t_{dec}, and the sampling frequency, f_s. Between these relevant proposals, a time-domain differential scheme uses the instantaneous power concept to implement the well-know logics 1-out-of-1 and 2-out-of-2 [3]. This function provides a minimum fault detection time of one-eighth of a cycle with suitable performance for different adverse scenarios. However, the presence of the decaying component and noise can slightly degrade its accuracy. In order to implement the same tripping logics, the Park's transformation, directly applied on the currents samples, allows the function to operate in 1,25 ms. However, this approach can only be applied to circuit breakers with three-pole operation [4]. The same problem is experienced by the superimposed currents-based method proposed by [5], whose accuracy is widely proved, but whose mathematical approach prevents the phase segregation.

TABLE I: Relevant Busbar Protection Schemes in last years

Reference	Method	t_{dec} (ms)	f_s (kHz)
[12]	Relevance Vector Machine	20	1
[5]	Superimposed Currents	2,5	4
[7]	Alienation Concept	–	5
[13]	Logistic Regression	23	1
[14]	Support Vector Machine	20,7	2,5
[6]	Partial Operating Current	4,4	10
[15]	Alpha Plane	5	4
[8]	Wavelet Transformation	0,26	15,36
[10]	Traveling Waves	2	8
[9]	Traveling Waves	0,5	60
[3]	Instantaneous Power	2,08	3,84
[4]	Park's Transformation	1,25	4
[11]	Mathematical Morphology	0,35	40
[16]	Alpha Plane	–	0,96

The strategy proposed by [6] calculates a partial operating current from those contributions above a minimum threshold. This algorithm can allow the operation of relay in 4,4 ms, but a high fault resistance can delay it. Also, the evolution of an external fault into the protection zone could be recognize only after one cycle. On the hand, [7] improved the percentage differential protection for a current transformer (CT) saturation scenario, through the determination of a coefficient to detect the non-similarity between saturated and non-saturated current signals.

Moreover, transient-based methods as wavelet transformation [8], traveling waves [9], [10], and mathematical morphology [11] were recently used for developing new busbar protection functions. This approach provides decision times less than 1 ms, but they need high sampling frequencies and the performance might be limited in front of transients attenuation. On the other hand, the machine learning-based approach provides high accuracy for fault identification at the cost of a large training data. That leads to a larger response time including the training process [12]–[14].

The generalized alpha plane (GAP) technique was originally

Francis A. Moreno Vásquez and Kleber M. Silva are with the University of Brasília, Brasília, Brazil (francisarody@unb.br, klebermelo@unb.br).

Paper submitted to the International Conference on Power Systems Transients (IPST2021) in Belo Horizonte, Brazil June 6-10, 2021.

formulated for protection of multi-terminal transmission lines [17], but it was already tested by [15] for low-impedance busbar protection purpose. This method consists of replacing the actual currents of all circuits by two equivalent ones, ensuring the preservation of the original differential and restraint currents. Based on this principle, the most recent method [16] modifies the original formulation to have control over the internal fault settlement region. Its potential was proved for transmission lines, power transformers and busbar protection. In turn, an alternative generalized alpha plane (AGAP) was proposed by [18] to apply in any n-terminal apparatus, but it has not yet been fully tested as a busbar protection function.

In this context, the first objective of this paper is to assess the application of a generalized alpha plane approach [17] to busbar protection. Although this method has already been adopted by [15] for a busbar application, a thorough assessment of this element reveals some challenges that were not identified in such paper, that can lead to the delay or maloperation of the function. On the other hand, once the potential of the strategy formulated by [16] was already demonstrated for busbar protection, this paper assesses the simple mathematical formulation of alternative generalized alpha plane-based technique proposed in [18] and its superiority is discussed in relation to original GAP, as well as to cited papers. The obtained results brings up the superiority of the alternative strategy in terms of response time for internal faults, even with different fault resistances and fault inception angles, suitable stability in front of external faults with CT saturation, and reliability in front of evolving external-to-internal faults.

II. Original Generalized Alpha Plane

The traditional current-based differential busbar protection establishes that, in normal operation conditions, the sum of incoming currents is equal to sum of outgoing currents, i.e., the differential current, $\bar{I}_{dif}$, is zero. Otherwise, if a fault occurs in bus zone, all currents flow into busbar and $\bar{I}_{dif}$ has a non-zero value. In this case, $\bar{I}_{dif}$ increases abruptly and an operation condition is declared after this signal becoming higher than a restraint current, $\bar{I}_{res}$. These two signals can be expressed, respectively, by:

$$\bar{I}_{dif} = \sum_{n=1}^{N} \bar{I}_n = I_{dif,re} + jI_{dif,im}, \tag{1}$$

$$I_{res} = \sum_{n=1}^{N} |\bar{I}_n| \tag{2}$$

where $\bar{I}_n$ is the actual current phasor in each circuit, n, and $I_{dif,re}$, $I_{dif,im}$ are the real and imaginary parts of differential current phasor, respectively. Also, a low-impedance differential element must consider the CT saturation as a critical point in order to avoid false operations in front of severe external faults. In that sense, I_{res} can be reinforced by second harmonic current, I_n^{2h}, which is a natural component of a saturated signal, so it can be finally expressed by:

$$I_{res} = \sum_{n=1}^{N} |\bar{I}_n| + f_{ext}.\sum_{n=1}^{N} |I_n^{2h}|, \tag{3}$$

where f_{ext} is a flag that indicates the recognition of fault as an external one, and acquires a logical level 1 (one) if the following condition is fulfilled during 4 ms:

$$|\bar{I}_{dif}| < 0.5.I_{res}. \tag{4}$$

The objective of generalized alpha plane method is to map the actual currents of bays connected to busbar throught two equivalent currents, $\bar{I}_N$ and $\bar{I}_M$. This substitution must ensure that the actual $\bar{I}_{dif}$ and I_{res} obtained from Eq. (1) and (3) be faithfully represented by the corresponding signals obtained from $\bar{I}_N$ and $\bar{I}_M$, as described in Eq. (5) and (6):

$$\bar{I}_{dif} = \bar{I}_M + \bar{I}_N \tag{5}$$

$$I_{res} = |\bar{I}_M| + |\bar{I}_N|. \tag{6}$$

In order to better illustrate that, the system illustrated in Fig. 5 was adopted to be similar to the single bus system, illustrated in Fig. 1. For that, the transmission lines TL1, TL2, and TL3, as well as the transformers, TF1 and TF2, were all connected to Bus 1, and the transmission line, TL4, was disconnected from the system. From that, the bays currents $\bar{I}_1$, $\bar{I}_2$, $\bar{I}_3$, $\bar{I}_4$ and $\bar{I}_5$ are replaced by $\bar{I}_M$ and $\bar{I}_N$, as in Fig. 1. Also, they can be visualized in a polar diagram in Figs. 2(a) and 2(b), respectively. It must be cited that this plane was also be used in [19] for discriminating external from internal faults through the calculation of the angles between these currents phasors. Now, for determination of the real and imaginary parts of $\bar{I}_M$ and $\bar{I}_N$, it is necessary to define the magnitude and the angle of $\bar{I}_{dif}$ and I_{res}. However, the argument of I_{res} does not exist, thus this missing parameter needs to be estimated for fully solving the equations system.

At this point, it is convenient to remember that, in case of an external fault with CT saturation, the current of this faulted circuit represents a major portion of the differential current. In other words, the current in the circuit where external fault occurs may have the highest projection on the differential current, I_{dif}. This idea was extended to internal faults, and the individual projection of each circuit is estimated by:

$$R_n = Re\{\bar{I}_n.\bar{I}_{dif}^*\}. \tag{7}$$

The proposal of [20] was to attribute the angle, β, of the current with the highest projection on I_{dif} to the current $\bar{I}_N$. In the example, it was found that $\bar{I}_3$ has the highest projection once the angle between $\bar{I}_N$ and $\bar{I}_{dif}$ is exactly the angle between $\bar{I}_3$ and $\bar{I}_{dif}$, as observed in Fig. 2(a) and 2(b). The differential current is then shifted for the convenience of subsequent calculations, so this new signal, I_X, is defined as

$$\bar{I}_X = \bar{I}_{dif}.1\angle(-\beta) \tag{8}$$

in such a way that $\bar{I}_M$ and $\bar{I}_N$ be finally calculated by

$$\bar{I}_M = \left\{ \frac{I_{X,im}^2 - [I_{res} - I_{X,re}]^2}{2[I_{res} - \bar{I}_{X,re}]} + jI_{X,im} \right\}.1\angle\beta \tag{9}$$

$$\bar{I}_N = (I_{res} - |\bar{I}_M|).1\angle\beta \tag{10}$$

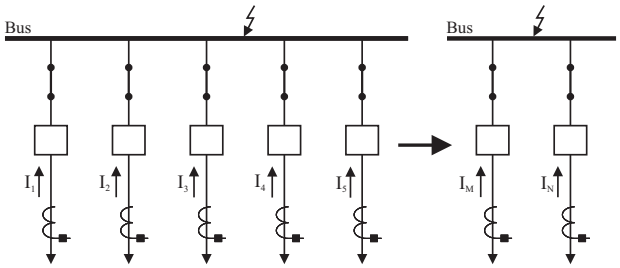

Fig. 1: Substitution of actual currents by alpha plane equivalent currents.

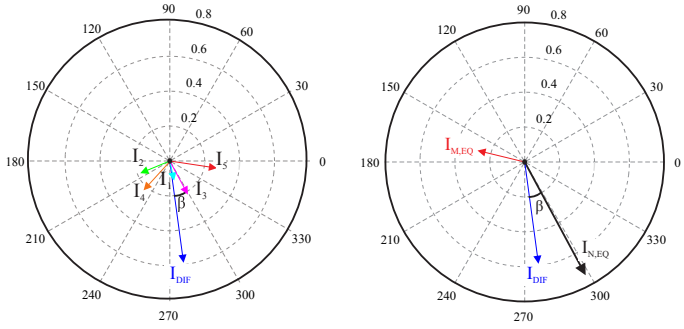

(a) (b)

Fig. 2: Polar representation of currents before changing of reference current. a) Actual currents; b) Equivalent currents.

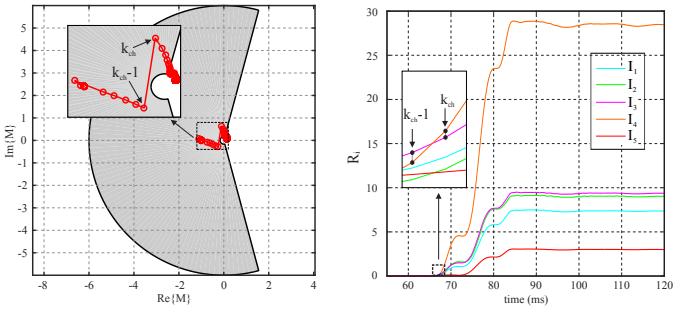

(a) (b)

Fig. 3: Reference current changing. a) Alpha plane response, b)Time domain response.

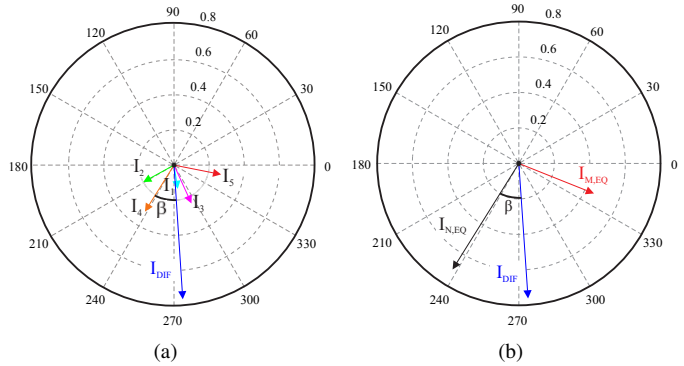

(a) (b)

Fig. 4: Polar representation of currents after changing of reference current. a) Actual currents; b) Equivalent currents.

The transient response in alpha plane is then visualized in Fig. 3(a) and it is obtained by computing the currents ratio, $\Gamma = \bar{I}_M/\bar{I}_N$ [21]. Here, the shaded area indicates the restraint region and the operation region is outside it. Undoubtedly, the choice of highest current projection on differential current as reference is absolutely understandable and, in principle, there is no reason to refute this strategy.

However, it is possible to note in Fig. 3(a) an abrupt change in the trajectory of Γ, what can be interpreted as an instability or a delay in the trip command sending once the mapped Γ would not leave the restraint region directly. It can be better visualized in the zoomed region of Fig. 3(b) that there is a change in the current reference in instant k_{ch}, i.e., from the fault inception until instant $(k_{ch}-1)$, the current $\bar{I}_3$ has the highest projection, but subsequently the current $\bar{I}_4$ becomes higher. Consequently, the equivalent current, $\bar{I}_N$ be now aligned with this current, as observed in Figs. 4(a) and 4(b). Its for this reason that, despite this method has given good responses in commercial relays for multiterminal transmission line protection, its application on differential busbar protection could be limited. That is because of a higher probability of reference permutation during transient period due to the great number of circuits connected to the busbar. On the other hand, it is possible that I_{res} and $\bar{I}_{X,re}$ be approximately equal, so the value of $\bar{I}_{M,ref}$ would tend to very high values, making the method unsuitable. To get around this problem, the original results shown in [15] suggests that Γ is forced to be zero in this case.

III. Modified Generalized Alpha Plane Formulation

In order to improve the busbar differential protection by using the original alpha plane formulation, [18] proposed a modified version (AGAP) where the differential and restraint currents can be now calculated by:

$$\bar{I}_{dif} = \bar{I}_M + \bar{I}_N, \quad (11)$$

$$\bar{I}_{res} = \bar{I}_M - \bar{I}_N. \quad (12)$$

These equations can be also expressed as

$$I_{dif,re} + jI_{dif,im} = I_{M,re} + jI_{M,im} + I_{N,re} + jI_{N,im}, \quad (13)$$

$$I_{res,re} + jI_{res,im} = I_{M,re} + jI_{M,im} - (I_{N,re} + jI_{N,im}). \quad (14)$$

The condition for validating the alternative method is that $\bar{I}_{dif}$ and $\bar{I}_{res}$, now calculated from $\bar{I}_M$ and $\bar{I}_N$, be equivalent to those obtained from original current signals, as in Eq. (1) and Eq. (2), respectively. Once this original restraint current is defined from absolute values, the imaginary part of equivalent $\bar{I}_{res}$ must be zero. Through the mathematical treatment of these equations, it can be obtained that:

$$\bar{I}_M = 0.5[\bar{I}_{dif} + k_{res}.\bar{I}_{res}], \quad (15)$$

$$\bar{I}_N = 0.5[\bar{I}_{dif} - k_{res}.\bar{I}_{res}]. \quad (16)$$

where, k_{res} is the slope whose value is suitably adjusted to this formulation. As previously explained, the original technique gives a determined and consistent linear system of equations with one degree of freedom, so the missing value is estimated. Contrarily, the restraint signal calculus in AGAP element can be directly calculated from phasor quantities. That means that the

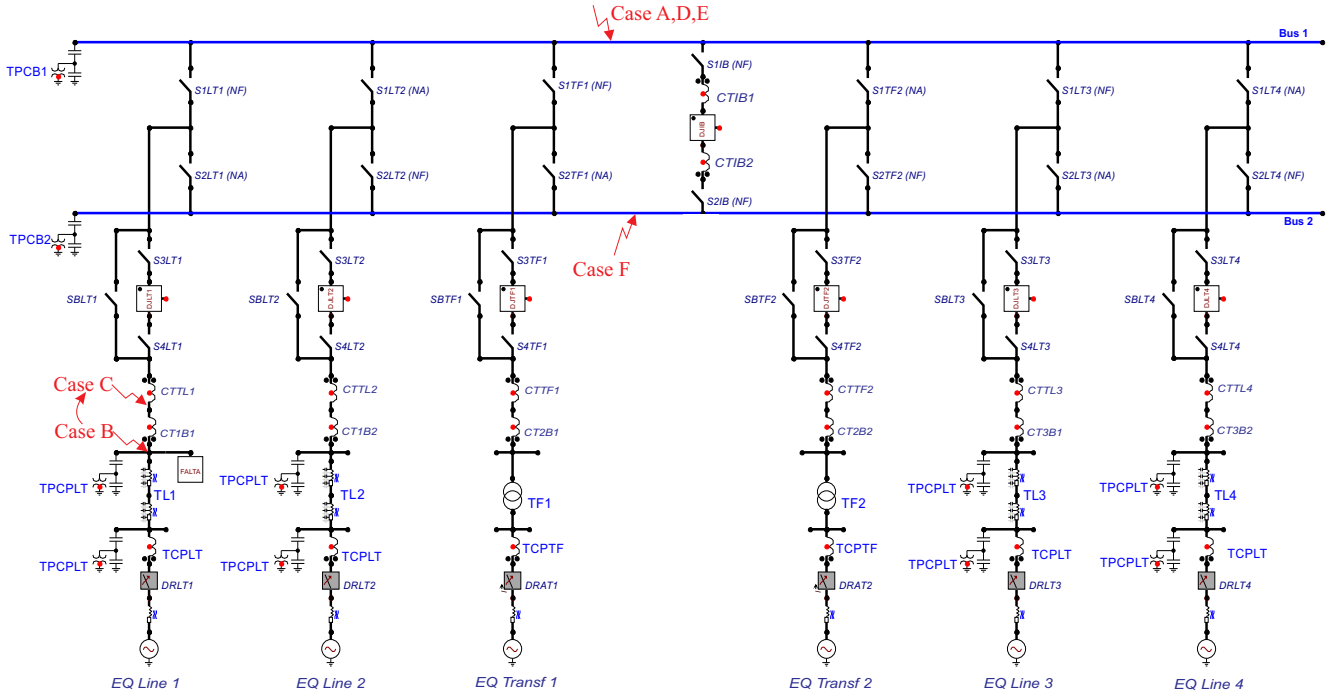

Fig. 5: Simulated power system.

algorithm is mathematically simpler once no reference current estimation process is needed to determine the angle between I_N and $\bar{I}_{dif}$. Likewise, the restraint signal can be also reinforced with second harmonic component of current, but in this case, this signal is expressed as

$$I_{res} = k_{res} \sum_{n=1}^{N} |\bar{I}_n| + f_{ext}.k_h|\bar{I}_n^{2h}| \tag{17}$$

where k_h is a factor to be applied only in the harmonic component in order to suitably increase the restraint current for avoiding false trip in case of severe external faults. Again, the restraint current obtained from $\bar{I}_M$ and $\bar{I}_N$ must be equal to I_{res} calculated from Eq. (17).

IV. Results and Discussion

In order to fully test the described techniques, various faults scenarios were simulated in a 230 kV/60Hz power system, modeled in ATPdraw program, as shown in Fig. 5. The topology of the substation is double bus and single breaker with five disconnect switches whose principal characteristics are its complexity and dynamic reconfiguration. In this power system, the transmission lines TL1 and TL3, and the power transformer TF1 are connected to Bus 1. In turn, the transmission lines TL2 and TL4, as well as the power transformer, TF2, are connected to Bus 2. In this busbar topology, both of buses are energized and interconnected through a tie breaker. The two CTs located in both sides of this circuit breaker are installed in such a way to avoid a dead zone, based on their polarities. That means that CTIB2 on Bus 2 side measures the current entering into Bus 1. Analogously, CTIB1 on Bus 1 side measures the current entering into Bus 2. Thus, an adaptive logic of bus zone selection must be implemented in parallel with protection logic to recognize these connections. Once this item is out of the focus of this work, the reader can better understand this logic in the document drafted by IEEE Power System Relaying Committee in [22]. Also, the model of CTs is reported in [23]. The current signals obtained from ATPDraw simulation with a time step equal to $1\mu s$ pass through an third-order anti-aliasing Butterworth filter. After that, the signals are sampled at 64 samples per cycle, corresponding to a sampling frequency of 3840 Hz. In order to carry out the simulations, the current phasors are estimated by using the modified cosine filter [24], the value of k_{res} is set to be 0.09 and k_h is 10. These factors was rigorously tested for several fault scenarios, in such a way to guarantee that internal faults could be recognized even with high fault resistances, or for critical fault angles. On the other hand, k_h provides robustness and tries to maintain the locus close to (-1,0), thus inside the restrain region in case of external faults with high saturation degree. Firstly, individual cases as internal fault, external fault with CT saturation, evolving fault, as well as internal fault with CT saturation and internal fault with noisy current signals were simulated. The results for these cases are presented through the alpha plane as well as the individual currents phasors variations with time. After that, the algorithms are tested for internal faults with different fault resistances, and finally a parametric sensitivity analysis is carried out, considering both internal and evolving faults with CT saturation.

A. Internal fault

In this case, a three phase internal fault is applied at 80 ms at Bus 1. The trajectories of Γ for original and alternative generalized alpha plane technique are shown in Fig. 6(a) and 6(b), respectively. It is possible to clearly observe again the reference current permutation phenomena for original GAP, contrarily to AGAP method which gives a more direct and well behaved trajectory. The Fig. 7 helps to visualize that the reference current changes during transient period in the three phases. Especially, it can be noticed in GAP method that, in phase C, this permutation occurs twice between the current measured from CT1B2 and the CT installed in the bay of the transformer TF1. For this reason, the trajectory of Γ changes even being outside the restrain region.

The time necessary to Γ leaves the restrain region for each phase is indicated in both of figures. As observed, the AGAP strategy needs only 0.98 ms after fault inception to go out from restraint region, contrarily to original GAP which requires a minimum time of 2.81 ms. At this point, it is appropriate to clarify that this first sample outside of restraint region would be the beginning of counting of any trip logic chosen for definitely recognizing the fault and to send the trip command to the circuit breaker. For example, [25] cites a commercial relay to 3 ms to in fact identify that the fault occurred within the bus protection zone. Likewise, [1] suggests a complete quarter cycle to take the same decision.

B. External fault with CT saturation

Here, an external fault, phase A to earth, AG, in transmission line TL1 at 80 ms is simulated. In order to obtain a severe degree CT saturation, the burden of CT was suitably adjusted. As expected, the current ratio trajectory in both of methods do not leave the restraint region, as shown in Fig. 8(a) and 8(b), respectively. Nevertheless, it is possible to observe a greater displacement of Γ with original GAP, approaching restraint region limits, as a result of changing of reference current. It can be also explained by observing the Fig. 9, where it can be noticed that during transient period, the current of bay TL1 becomes higher than CT1B2, leading to a reference current changing in original GAP. After that, there is new permutations between these two signals, leading to new changes of locus trajectory in alpha plane. On its turn, the alternative function allows to keep the locus of Γ close to (-1,0), i.e., it is more robust. In any case, it is important to underscore the helpfulness of additional reinforcement of restraint signals with estimated second harmonic phasors.

C. Evolving external-to-internal fault

A severe AG external fault at 80 ms takes place causing the saturation of CT, and it evolves to an internal ABG fault in 103 ms. Figs. 10(a) and 10(b) shows the trajectory of Γ for original GAP and AGAP. It is clear the later provides a well behaved trajectory of Γ with the AGAP element, which leaves the restraint region smoothly. On the contrary, the original GAP features a change of the current reference that may be interpreted as a poor stability characteristic.

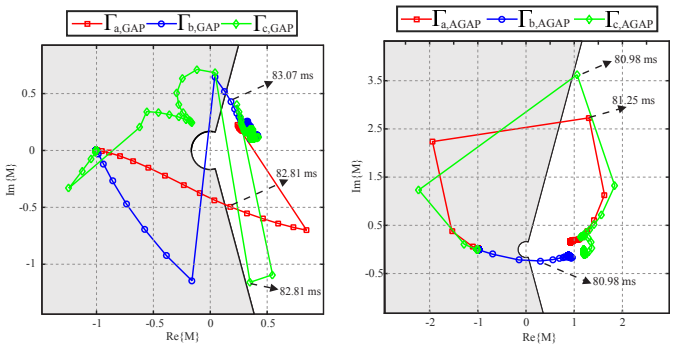

(a) (b)

Fig. 6: Three-phase internal short circuit. a) Original GAP formulation b) AGAP.

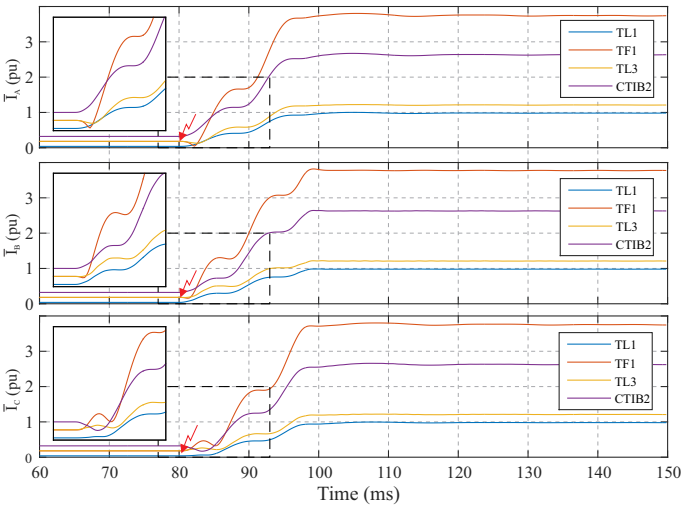

Fig. 7: Estimated phasors of phase currents in Bus 1 for an internal fault in 80 ms.

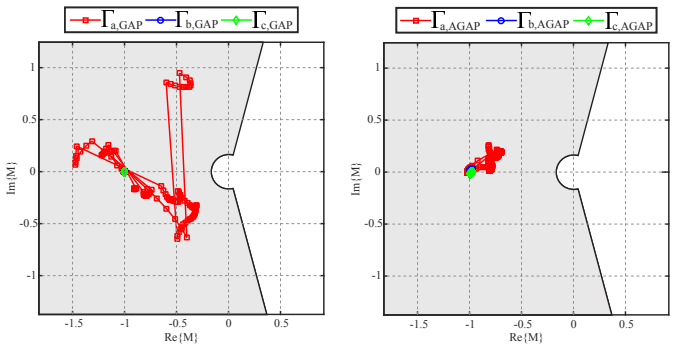

(a) (b)

Fig. 8: External fault with CT saturation. a) Original GAP formulation b) AGAP.

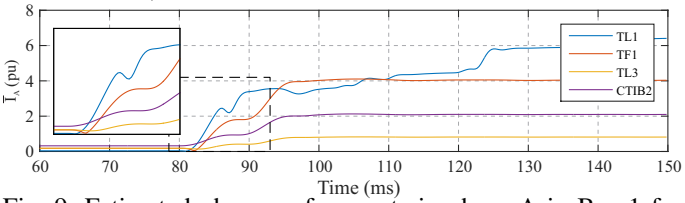

Fig. 9: Estimated phasors of currents in phase A in Bus 1 for an external fault in 80 ms with CT saturation.

The Fig. 11 shows the variation of currents of phase A and B after the external fault instant. Here, it can be identified that the evolution of fault within protection zone is recognized by the alternative AGAP at 121,35 ms in phase A, when the contribution of TL1 bay becomes lower than the other currents. By the way, these delay is caused by the size of the sampling windows of the phasor estimation method. On the other hand, the currents on phase B rapidly increase only after the internal fault instant. Nevertheless, it is convenient to note that the time necessary to have the first sample outside the restraint region in initially involved phase A with original GAP, 14.70 ms, is some milliseconds lesser than AGAP technique, 18.35 ms. Even so, by observing the instant when the first sample of Γ is outside the restraint region of initially non involved phase B, the AGAP method is equally better than original formulation. It means that for both of techniques, there is a considerable delay for the phase initially involved in short circuit, but when it evolves to an internal fault and include other phase, the AGAP function still gives a quicker response if compared with original GAP.

D. Internal fault with CT saturation

In this case, a phase-to-ground fault (AG) is simulated in Bus 1, considering the saturation of the same current transformer of case IV-B. The Fig. 12 show the response of original and alternative alpha plane-based methods. Here, the AGAP method has the first sample outside the restrain region at 81,51 ms. It turn, the original GAP provides this sample at 83,33 ms. On the other hand, it can be seen in Fig. 13 that the phasor of current signal is similar to a scenario without CT saturation. In conclusion, the CT saturation during an internal fault is not critical to any of methods, but either way the alternative GAP technique is faster.

E. Internal fault with noised current signals

In this case, an internal BCG fault occurs in Bus 1 and a white random noise was added to simulated signals with a signal-to-noise ratio (SNR) per sample of 40 dB. It can be noted in Fig. 14 that the trajectory of locus for both of methods is similar to an internal fault case, as in subsection IV-A. In fact, the phasors of Fig. 15 are not distorted. This is because the signal conditioning process of current signals includes a anti-aliasing Butterworth low-pass filter to eliminate high frequency components. Finally, the noise has not effect on the performance of alpha plane-based methods.

F. Internal fault with fault resistance

In order to show the sensitivity of original and alternative methods, it was simulated a one phase internal fault at 100 ms with different values of fault resistance between 0 Ω and 400 Ω. In this case, it was considered appropriate to take the last sample of simulation, because it certainly represents the stabilization point of Γ, i.e., when short-circuit reaches its steady-state value. From Fig. 16, it can be noted that as fault resistance increases, the trajectory of Γ with GAP approaches to restraint region.

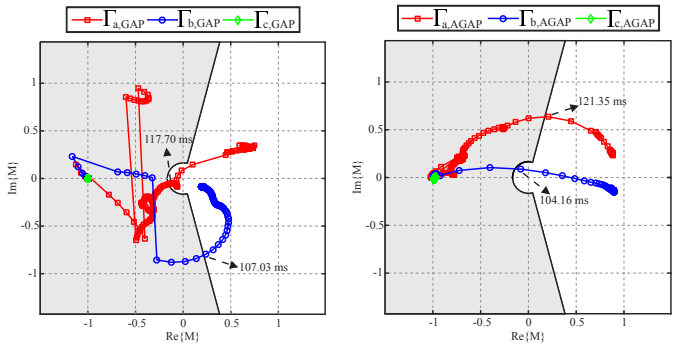

(a) (b)

Fig. 10: Evolving external-to-internal fault. a) Original GAP formulation b) AGAP.

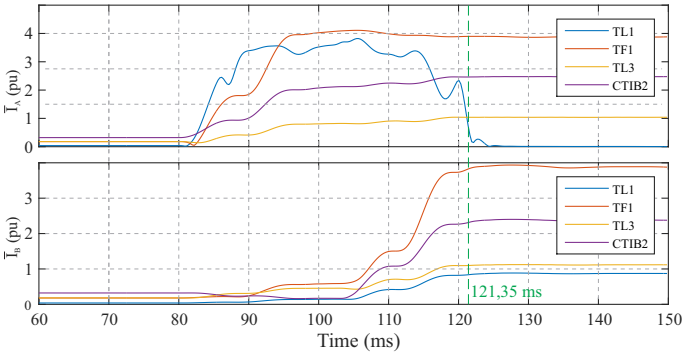

Fig. 11: Estimated phasors of currents in phases A and B, in Bus 1 for an evolving fault with CT saturation.

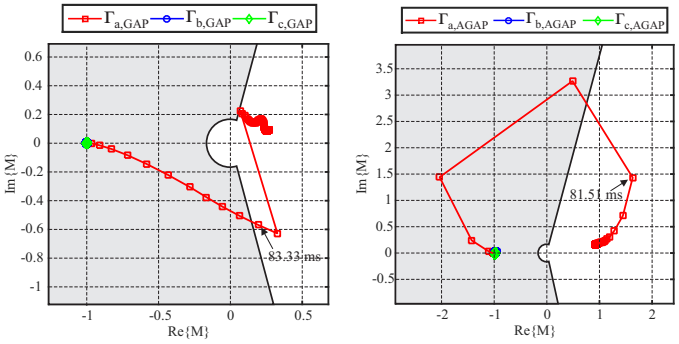

(a) (b)

Fig. 12: Internal fault with CT saturation a) Original GAP formulation b) AGAP.

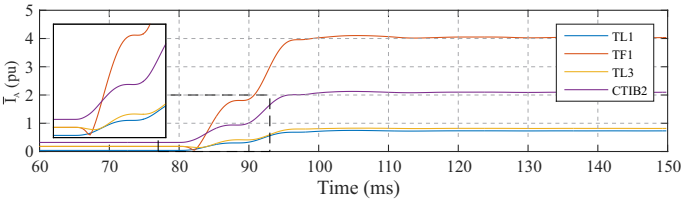

Fig. 13: Estimated phasors of currents in phases A, in Bus 1 for an internal fault with CT saturation.

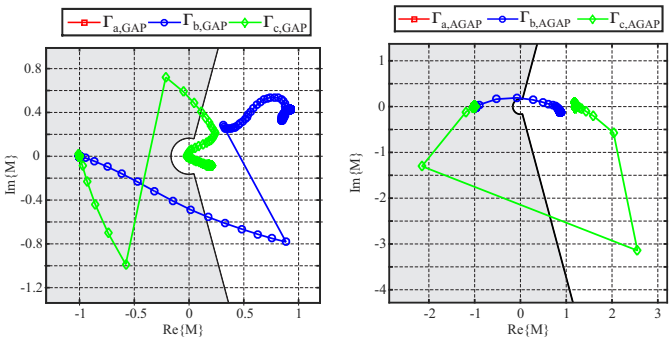

(a) (b)

Fig. 14: Internal fault with noised current signals. a) Original GAP formulation b) AGAP.

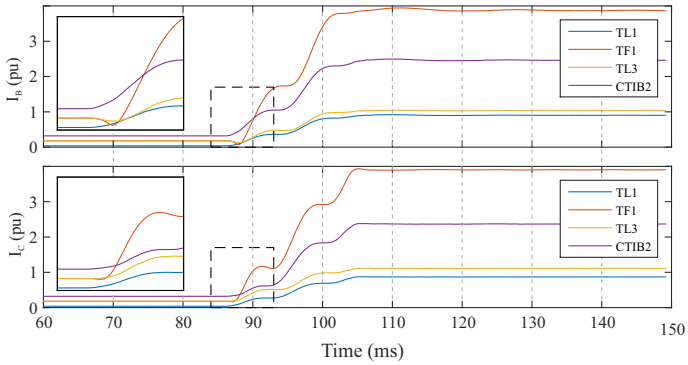

Fig. 15: Estimated phasors of currents in phases B and C, in Bus 1, for an internal fault with noise of 40 dB in current signals.

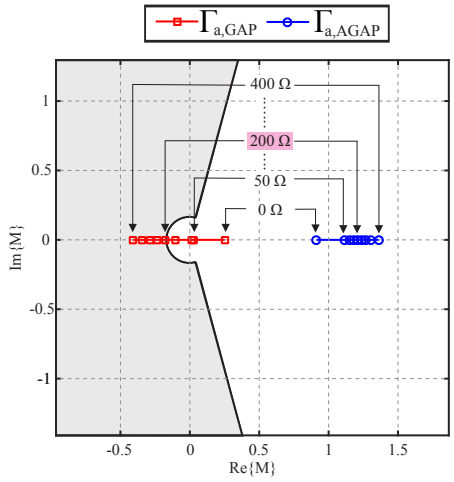

Fig. 16: Fault resistance impact in GAP and AGAP methods.

Also, when resistance becomes 200 Ω it stabilizes inside the restraint region, i.e., the original GAP would not be capable to send a trip command. Conversely, the AGAP element performs a contrary trajectory, i.e., Γ moves away from restraint region as fault resistance increases. It is important to point out that this trajectory with AGAP is not mandatory but, in any case, it is guaranteed that Γ will always establish outside the restraint region, making this technique immune to high values of fault resistance.

G. Parametric Sensitivity Analysis

With the purpose of proving the superiority of AGAP method over the original algorithm, it is performed a massive data analysis through the simulation of internal faults and evolving external-to-internal faults. In this analysis, the criteria is the time necessary for Γ moving outside the restrain region. In this regard, the fault resistance of ground faults (R_G), the resistance between phases of ungrounded faults (R_f), the angle of fault inception (θ) and the fault type (involved phase) are varied according to Table II. Also, in case of evolving faults, it was considered an initial external AG fault with $R_g = 150\Omega$. The results are summarized in Table III in terms of mean time, μ, and standard deviation, σ. It can be observed from Figs. 17(a) and 17(b) that modified technique, AGAP, can be several times faster than GAP for leaving the restraint region in case of internal and evolving faults. It can be noted a greater dispersion when evolving faults involves only the phase A, but the superiority of AGAP element is still visible.

TABLE II: Fault parameters used in the massive data analysis

Parameter	Value
R_G	0, 25, 50, 75 and 100 Ω
R_F	0, 5, 10, 15 and 20 Ω
θ	0°, 30°, 60°, . . . , 150° and 180°
Fault Type	AG, BG, CG, AB, BC, CA, ABG, BCG, CAG and ABC

TABLE III: Statistics of the operating times in milliseconds

Measure	Internal Faults	Evolving Faults
μ_{AGAP}	1.1228	1.2158
σ_{AGAP}	0.5919	0.7058
μ_{GAP}	6.2173	6.2842
σ_{GAP}	4.6399	4.2835

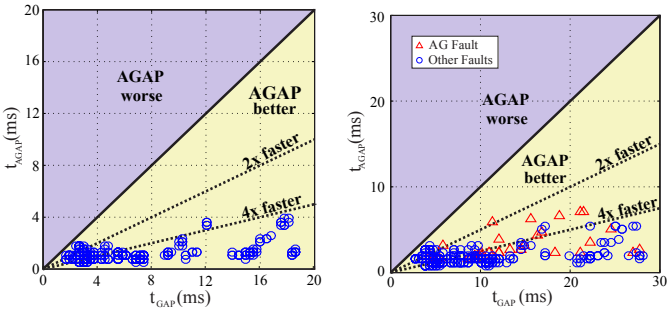

(a) (b)

Fig. 17: Massive data analysis. a) Internal faults b) Evolving external-to-internal faults.

V. Conclusion

This paper brings out that, despite the relevance of original GAP element for protection of multi-terminal transmission lines, this approach faces a harder challenge when tested for differential busbar protection. That is due to current reference switching during fault transient period, causing a delay in relay operation. In that sense, the AGAP method provides

results more consonants with those expected for a busbar protection algorithm. The results shows that besides the reduced time to leave the restraint region in case of internal faults, the current ratio trajectory is well behaved even in front of severe external faults. Moreover, the reliability of AGAP formulation was successfully proven in front evolving faults. On the other hand, the fault resistance does not represent a problem once the trajectory always stabilizes outside the restraint region. If compared with references in Table I, the high accuracy of the alternative AGAP is proved for different fault scenarios, providing an average decision time of 1,12 ms for internal faults. This time is only greater than transient-based techniques. By the way, once the alternative AGAP method does not need a high sampling frequency, its performance is not compromised in presence of noisy signals. On the other hand, in contrast with another methods with a great delay for recognizing evolving faults, the alternative method provides high reliability with an average fault recognition time of only 6,21 ms after the evolution. Moreover, this method is robust in front of severe external faults, by contrast with original GAP method, whose locus displacement could approximate the limit of restraint region. Finally, its on-chip implementation could be also possible without considerable complications because of its mathematical simplicity and similarity with the commercial GAP function.

REFERENCES

[1] H. J. A. Ferrer and E. O. Schweitzer., *Modern Solutions for Protection, Control and Monitoring of Electric Power Systems*. Pullman USA: Schweitzer Engineering Laboratories, Inc., 2010.

[2] K. Behrendt, D. Costello, and S. E. Zocholl, "Considerations for using high-impedance or low-impedance relays for bus differential protection," *IEEE 63rd Annual Conference for Protective Relay Engineers*, pp. 1–15, March 2010.

[3] F. A. M. Vásquez and K. M. Silva, "Instantaneous-power-based busbar numerical differential protection," *IEEE Transactions on Power Delivery*, vol. 34, no. 2, pp. 616–626, 2019.

[4] S. Jena and B. Bhalja, "Sampled value-based bus zone protection scheme with dq-components," *IET Generation, Transmission & Distribution*, vol. 14, pp. 4520–4528(8), October 2020. [Online]. Available: https://digital-library.theiet.org/content/journals/10.1049/iet-gtd.2019.1649

[5] S. Song and G. Zou, "A novel busbar protection method based on polarity comparison of superimposed current," *IEEE Transactions on Power Delivery*, vol. 30, no. 4, pp. 1914–1922, 2015.

[6] M. Hossain, I. Leevongwat, and P. Rastgoufard, "Partial operating current characteristics to discriminate internal and external faults of differential protection zones during ct saturation," *IET Generation, Transmission Distribution*, vol. 12, no. 2, pp. 379–387, 2018.

[7] R. A. Allah, "Adaptive busbar differential relaying scheme during saturation period of current transformers based on alienation concept," *IET Generation, Transmission Distribution*, vol. 10, no. 15, pp. 3803–3815, 2016.

[8] K. M. Silva, A. M. P. Escudero, F. V. Lopes, and F. B. Costa, "A wavelet-based busbar differential protection," *IEEE Transactions on Power Delivery*, vol. 33, no. 3, pp. 1194–1203, June 2018.

[9] H. Wu, X. Dong, and Q. Wang, "A new principle for initial traveling wave active power differential busbar protection," *IEEE Access*, vol. 7, pp. 70 495–70 512, 2019.

[10] S.Jena, "Initial travelling wavefront-based bus zone protection scheme," *IET Generation, Transmission & Distribution*, vol. 13, pp. 3216–3229(13), August 2019. [Online]. Available: https://digital-library.theiet.org/content/journals/10.1049/iet-gtd.2018.6155

[11] M. Lashgari, "Fast transient-based detection of busbar faults employing improved morphological gradient," *IET Generation, Transmission & Distribution*, vol. 14, pp. 1458–1466(8), April 2020. [Online]. Available: https://digital-library.theiet.org/content/journals/10.1049/iet-gtd.2019.0119

[12] N. G. Chothani and B. R. Bhalja, "A new algorithm for busbar fault zone identification using relevance vector machine," *Electric Power Components and Systems*, vol. 44, no. 2, pp. 193–205, January 2015.

[13] S. Jena and B. R. Bhalja, "Development of a new fault zone identification scheme for busbar using logistic regression classifier," *IET Generation, Transmission Distribution*, vol. 11, no. 1, pp. 174–184, 2017.

[14] M. Gil and A. A. Abdoos, "Intelligent busbar protection scheme based on combination of support vector machine and s-transform," *IET Generation, Transmission Distribution*, vol. 11, no. 8, pp. 2056–2064, 2017.

[15] S. Jena and B. R. Bhalja, "Numerical busbar differential protection using generalised alpha plane," *IET Generation, Transmission Distribution*, vol. 12, no. 1, pp. 227–234, 2018.

[16] R. G. Bainy and K. M. Silva, "Enhanced generalized alpha plane for numerical differential protection applications," *IEEE Transactions on Power Delivery*, pp. 1–1, 2020.

[17] G. B. J. Roberts, D. Tziouvaras and H. Altuve, "The effect of multiprinciple line protection on dependability and security," in *proceedings of the 55th Annual Georgia Tech Protective Relaying Conference, Atlanta, GA*, May 2001, pp. 1–25.

[18] K. M. Silva and R. G. Bainy, "Generalized alpha plane for numerical differential protection applications," *IEEE Transactions on Power Delivery*, vol. 31, no. 6, pp. 2565–2566, Dec 2016.

[19] *B-PRO 8700 Bus Protection Relay, User Manual*, ERLPhase Power Technologies Ltd., Dez. 2016.

[20] H. Miller, J. Burger, N. Fischer, and B. Kasztenny, "Modern line current differential protection solutions," in *2010 63rd Annual Conference for Protective Relay Engineers*, March 2010, pp. 1–25.

[21] V. N. Warrington, *Protective Relays: Their Theory and Practice*, ser. Protective relays. Chapman and Hall, 1962.

[22] *IEEE Std C37.234 - Guide for Protective Relay Applications to Power System Buses*, IEEE Power & Energy Society, Power System Relaying Committee, 2009.

[23] *EMTP Reference Models for Transmission Line Relay Testing*, IEEE Power System Relaying Committee, 2004.

[24] D. G. Hart, D. Nosovel, and R. A. Smith, *Modified cosine filters*. U.S. Patent 6,154,687: November, 2000.

[25] G. Ziegler, *Numerical Differential Protection, Principles and Applications*. Wiley-VCH, 2012, vol. 2.